

Same-Sign Tetralepton Signature at Large Hadron Collider, and future pp Collider.

Eung Jin Chun,^a Sarif Khan,^{b,c} Sanjoy Mandal,^{d,e} Manimala Mitra,^{d,e} Sujay Shil^{d,e}

^a*Korea Institute for Advanced Study, Seoul 130-722, Korea*

^b*Institut für Theoretische Physik, Georg-August-Universität Göttingen, Friedrich-Hund-Platz 1, Göttingen, D-37077 Germany*

^c*Harish-Chandra Research Institute, Allahabad, India*

^d*Institute of Physics, Sachivalaya Marg, Bhubaneswar, Odisha 751005, India*

^e*Homi Bhabha National Institute, BARC Training School Complex, Anushakti Nagar, Mumbai 400094, India*

E-mail: ejchun@kias.re.kr, sarif.khan@uni-goettingen.de,
smandal@iopb.res.in, manimala@iopb.res.in, sujayshil1@gmail.com

ABSTRACT: We analyze a novel signature of the type II seesaw model - same-sign tetra-lepton signal arising from the mixing of neutral Higgs bosons and their subsequent decays to singly and doubly charged Higgs bosons. For this, we consider wide ranges of the triplet vacuum expectation value (vev) and Yukawa couplings, that are consistent with the observed neutrino masses and mixing as well as the LHC search limits. We find that a doubly charged Higgs boson with mass around 250 GeV and triplet vev around $10^{-4} - 10^{-2}$ GeV can give significantly large number of events through its decay to same-sign W gauge bosons at High-Luminosity LHC with 3000fb^{-1} of data. We also pursue the analysis for a future hadron collider with the c.m. energy of 100 TeV. Considering a heavy Higgs boson around 900 GeV and an intermediate region of the triplet vev, where both same-sign dilepton and gauge boson decays can occur, we identify a limited range of the parameters where the number of same-sign tetra-lepton events are as large as 1000.

Contents

1	Introduction	1
2	Model Description	3
3	Decay Modes and Experimental Constraints	5
4	Large triplet vev and same-sign tetra-lepton signature for $\sqrt{s} = 14$ TeV	9
5	Inclusive same-sign tetra-lepton signature for $\sqrt{s} = 100$ TeV	13
6	Conclusion	15

1 Introduction

After the discovery of the Standard Model (SM) Higgs boson, one of the key questions that still remains unexplained is the origin of light neutrino masses and mixings. A number of neutrino oscillation experiments have observed that the solar and atmospheric neutrino mass splittings are $\Delta m_{12}^2 \sim 10^{-5}$ eV² and $\Delta m_{13}^2 \sim 10^{-3}$ eV². The PMNS mixing angles are $\theta_{12} \sim 32^\circ$, $\theta_{23} \sim 45^\circ$, and $\theta_{13} \sim 9^\circ$ [1]. Once we include the right handed neutrinos in the theory, a Dirac mass term can be generated for light neutrinos. However, to generate eV neutrino masses, this requires a very large hierarchy of the Yukawa couplings $Y_\nu \sim \mathcal{O}(10^{-11})$ within the SM. The light neutrinos, being electromagnetic charge neutral, can be Majorana particle, and their masses can have a different origin compared to the other SM fermions. One of the profound mechanisms to generate Majorana masses of the light neutrinos is seesaw, where tiny eV masses of the Majorana neutrinos are generated from lepton number violating (LNV) $d = 5$ operator $LLHH/\Lambda$ [2, 3]. There can be different UV completed theories behind this operator, commonly known as, type-I, -II, and -III seesaw mechanisms. These different models accommodate extensions of the SM fermion/scalar contents by $SU(2)_L$ singlet fermions [4–10], $SU(2)_L$ triplet scalar boson [11–14], and $SU(2)_L$ triplet fermions [15], respectively. Among these, type-II seesaw model, where a triplet scalar field with the hypercharge $Y = +2$ is added to the SM, has an extended scalar sector. See [16–18] for the details of the Higgs spectrum. The bound from vacuum stability, perturbativity, and electroweak precision test has been studied in [19]. The neutral component of the triplet acquires a vacuum expectation value (vev) v_Δ , and generates eV scale neutrino masses through the Yukawa interaction between lepton doublets and triplet Higgs field. The same Yukawa interaction also have a large impact on the charged Higgs phenomenology in this model. The presence of a doubly charged Higgs, that can have distinct decay modes whose branching ratios are determined by the observed neutrino oscillation data [20], is the most

appealing feature of this model. Hence a discovery of this exotic particle will be a smoking gun signature of this model.

A number of searches have been carried out to look for the signature of the doubly charged Higgs at collider and non-collider experiments [20]. See [21] for Tevatron, and [22–34] for LHC, [35–37] for HE-LHC and future hadron colliders. Depending on the triplet vev, the doubly-charged Higgs boson can decay via distinguished decays modes. Assuming degenerate charged Higgs masses, it decays pre-dominantly to same-sign dileptons (gauge bosons) for $v_\Delta < (>) 10^{-4}$ GeV. For non-degenerate charged Higgs, in the intermediate range of triplet vev, the cascade decay to singly charged Higgs can also be dominant and has been explored in [22–24]. The CMS and ATLAS collaborations have searched for the same-sign dilepton final states, and constrained the mass of the doubly-charged Higgs as $M_{H^{\pm\pm}} > 820, 870$ GeV at 95% C.L. [38, 39] assuming $\text{Br}(H^{\pm\pm} \rightarrow \ell^\pm \ell^\pm) = 100\%$. The vector boson fusion channel, where the $H^{\pm\pm}$ is produced in association with two jets, gives relaxed constraints [40, 41]. The collider signatures and the discovery prospect of this scenario have been discussed in [42–44], and [45, 46]. Previous searches for $H^{\pm\pm}$ in the pair-production channel and their subsequent decays into same-sign leptons at LEP-II has put a constraint $M_{H^{\pm\pm}} > 97.3$ GeV at 95% C.L. [47]. For the earlier discussions on Higgs triplet model at a linear collider, see [48–52].

Most of the works in the literature explored di-lepton or gauge boson decay modes of the doubly charged Higgs, leading to multi-lepton final states. Due to the possible cascade decays of the charge neutral Higgs into a singly charged Higgs, and the cascade decay of a singly charged Higgs into a doubly charged Higgs, the model can also lead to a very unique signature, same-sign tetra-lepton final states. This has been first proposed in [53], and explored for the lower triplet vev, where di-lepton decay is pre-dominant. In this work, we consider a wide range of triplet vev, in particularly, focussing on gauge boson decay modes, and explore the signature for 14 TeV LHC. For higher range of triplet vev, as the LHC constraint on the mass of doubly charged Higgs is relatively relaxed, we therefore perform the analysis for lighter Higgs state, as low as $M_{H^{\pm\pm}} \sim 247$ GeV. In addition, we also consider a very high energy pp collider, that can operate with c.m.energy $\sqrt{s} = 100$ TeV, and explore this unique signature for a heavy doubly charged Higgs. We show that for heavier doubly charged Higgs, there is a very narrow region of triplet vev, which can accommodate significantly large $\mathcal{O}(10^3)$ same-sign tetra-lepton signatures.

Our paper is organized as follows: we briefly review the basics of the type-II seesaw model in Sec. 2. In Sec. 3, we discuss branching ratios of doubly and singly charged Higgs, and the relation between $H^{\pm\pm}$ and H^\pm decays. In Sec. 4, and in Sec. 5, we present the simulation of same-sign tetra-lepton signal at $\sqrt{s} = 14$ TeV LHC, and $\sqrt{s} = 100$ TeV. Finally, we present our conclusions in Sec. 6.

2 Model Description

One of the most simplest seesaw models is the type-II seesaw model [11–14], that, in addition to the SM particle contents, also contains one $SU(2)_L$ triplet Higgs field

$$\Delta = \begin{pmatrix} \frac{\Delta^+}{\sqrt{2}} & \Delta^{++} \\ \Delta^0 & -\frac{\Delta^+}{\sqrt{2}} \end{pmatrix} \sim (1, 3, 2). \quad (2.1)$$

The neutral components of the SM doublet (Φ) and triplet Higgs fields are denoted as $\Phi^0 = \frac{1}{\sqrt{2}}(\phi^0 + i\chi^0)$ and $\Delta^0 = \frac{1}{\sqrt{2}}(\delta^0 + i\eta^0)$, respectively. The neutral component of Δ acquires vev and generates Majorana masses for light neutrinos. We denote the vevs of ϕ^0 and δ^0 by v_Φ and v_Δ , where $v^2 = v_\Phi^2 + v_\Delta^2 = (246 \text{ GeV})^2$. The kinetic term for the triplet has the following form

$$\mathcal{L}_{\text{kin}}(\Delta) = \text{Tr}[(D_\mu \Delta)^\dagger (D^\mu \Delta)], \quad (2.2)$$

In the above, D_μ is the co-variant derivative $D_\mu \Delta = \partial_\mu \Delta + i\frac{g}{2}[\tau^a W_\mu^a, \Delta] + ig' B_\mu \Delta$. The new triplet scalar field Δ , being a triplet under $SU(2)_L$ interacts with the SM gauge bosons. In addition to the kinetic term, Δ has Yukawa interaction with the SM lepton doublet. The Yukawa interactions of Δ with the lepton fields are

$$\mathcal{L}_Y(\Phi, \Delta) = Y_\Delta \bar{L}_L^c i\tau_2 \Delta L_L + \text{h.c.}, \quad (2.3)$$

where Y_Δ is a 3×3 matrix and c denotes charge conjugation. The scalar potential of the Higgs fields Φ and Δ is

$$\begin{aligned} V(\Phi, \Delta) = & m_\Phi^2 \Phi^\dagger \Phi + \tilde{M}_\Delta^2 \text{Tr}(\Delta^\dagger \Delta) + \left(\mu \Phi^T i\tau_2 \Delta^\dagger \Phi + \text{h.c.} \right) + \frac{\lambda}{4} (\Phi^\dagger \Phi)^2 \\ & + \lambda_1 (\Phi^\dagger \Phi) \text{Tr}(\Delta^\dagger \Delta) + \lambda_2 \left[\text{Tr}(\Delta^\dagger \Delta) \right]^2 + \lambda_3 \text{Tr}[(\Delta^\dagger \Delta)^2] + \lambda_4 \Phi^\dagger \Delta \Delta^\dagger \Phi, \end{aligned} \quad (2.4)$$

where m_Φ and \tilde{M}_Δ are real parameters with mass dimension 1, and λ, λ_{1-4} are dimensionless quartic Higgs couplings. Note that, μ is the parameter with positive mass dimension. The triplet field Δ carries lepton number +2 and hence the Yukawa term conserves lepton number. However, the lepton number is violated 2-units by a non-zero μ . Therefore, together a non-zero μ and a non-zero Y_ν violate lepton number symmetry.

The scalar potential that generates scalar mass matrix, includes tri-linear as well as quartic couplings among the scalar fields. The scalar mass matrix, after diagonalization, generates seven physical Higgs states. They are: the charged Higgs bosons $H^{\pm\pm}, H^\pm$, and the neutral Higgs bosons h^0, H^0 and A^0 . The two charged scalar fields Φ^\pm of Φ and Δ^\pm of Δ mix to give singly-charged states H^\pm and the charged Goldstone χ^\pm bosons. Similarly, the mixing between the two CP-odd fields (χ^0 and η^0) gives rise to A^0 , and the neutral Goldstone boson ρ^0 . Finally, we obtain the SM Higgs boson (h) and a heavy Higgs boson (H) via the mixing of the two neutral CP-even states Φ^0 and δ^0 . For the detail description of the charged and neutral mass matrix, see [16].

The minimization conditions of the potential are

$$\frac{\partial V(\Phi, \Delta)}{\partial v_\Phi} = 0, \quad \frac{\partial V(\Phi, \Delta)}{\partial v_\Delta} = 0.$$

These give the following conditions for m_Φ^2, M^2 :

$$m_\Phi^2 = \frac{1}{2} \left[-\frac{v_\Phi^2 \lambda}{2} - v_\Delta^2 (\lambda_1 + \lambda_4) + 2\sqrt{2}\mu v_\Delta \right], \quad (2.5)$$

$$\tilde{M}^2 = M_\Delta^2 - \frac{1}{2} [2v_\Delta^2 (\lambda_2 + \lambda_3) + v_\Phi^2 (\lambda_1 + \lambda_4)], \text{ with } M_\Delta^2 \equiv \frac{v_\Phi^2 \mu}{\sqrt{2}v_\Delta}. \quad (2.6)$$

The diagonalization conditions for the neutral and charged scalar fields are,

$$\begin{aligned} \begin{pmatrix} \phi^\pm \\ \Delta^\pm \end{pmatrix} &= \begin{pmatrix} \cos \beta_\pm & -\sin \beta_\pm \\ \sin \beta_\pm & \cos \beta_\pm \end{pmatrix} \begin{pmatrix} \chi^\pm \\ H^\pm \end{pmatrix}, & \begin{pmatrix} \chi \\ \eta \end{pmatrix} &= \begin{pmatrix} \cos \beta_0 & -\sin \beta_0 \\ \sin \beta_0 & \cos \beta_0 \end{pmatrix} \begin{pmatrix} \rho^0 \\ A^0 \end{pmatrix}, \\ \begin{pmatrix} \phi^0 \\ \delta^0 \end{pmatrix} &= \begin{pmatrix} \cos \alpha & -\sin \alpha \\ \sin \alpha & \cos \alpha \end{pmatrix} \begin{pmatrix} h^0 \\ H^0 \end{pmatrix}, \end{aligned} \quad (2.7)$$

where the mixing angles

$$\tan \beta_\pm = \frac{\sqrt{2}v_\Delta}{v_\Phi}, \quad \tan \beta_0 = \frac{2v_\Delta}{v_\Phi}, \quad \tan 2\alpha = \frac{4v_\Delta}{v_\Phi} \frac{v_\Phi^2 (\lambda_1 + \lambda_4) - 2M_\Delta^2}{v_\Phi^2 \lambda - 2M_\Delta^2 - 4v_\Delta^2 (\lambda_2 + \lambda_3)}. \quad (2.8)$$

All these mixings being proportional to the ratio of $\frac{v_\Delta}{v_\Phi}$ is very small.

The physical masses of the doubly and singly charged Higgs bosons $H^{\pm\pm}$ and H^\pm can be written as

$$m_{H^{++}}^2 = M_\Delta^2 - v_\Delta^2 \lambda_3 - \frac{\lambda_4}{2} v_\Phi^2, \quad m_{H^\pm}^2 = \left(M_\Delta^2 - \frac{\lambda_4}{4} v_\Phi^2 \right) \left(1 + \frac{2v_\Delta^2}{v_\Phi^2} \right). \quad (2.9)$$

The CP-even and CP-odd neutral Higgs bosons h , and H have the physical masses

$$m_{h^0}^2 = \mathcal{T}_{11}^2 \cos^2 \alpha + \mathcal{T}_{22}^2 \sin^2 \alpha - \mathcal{T}_{12}^2 \sin 2\alpha, \quad (2.10)$$

$$m_{H^0}^2 = \mathcal{T}_{11}^2 \sin^2 \alpha + \mathcal{T}_{22}^2 \cos^2 \alpha + \mathcal{T}_{12}^2 \sin 2\alpha. \quad (2.11)$$

In the above \mathcal{T}_{11} , \mathcal{T}_{22} and \mathcal{T}_{12} have the following expressions:

$$\mathcal{T}_{11}^2 = \frac{v_\Phi^2 \lambda}{2}, \quad \mathcal{T}_{22}^2 = M_\Delta^2 + 2v_\Delta^2 (\lambda_2 + \lambda_3), \quad \mathcal{T}_{12}^2 = -\frac{2v_\Delta}{v_\Phi} M_\Delta^2 + v_\Phi v_\Delta (\lambda_1 + \lambda_4). \quad (2.12)$$

The CP-odd Higgs field A^0 has the following mass

$$m_A^2 = M_\Delta^2 \left(1 + \frac{4v_\Delta^2}{v_\Phi^2} \right), \quad \text{with } M_\Delta^2 = \frac{v_\Phi^2 \mu}{\sqrt{2}v_\Delta}. \quad (2.13)$$

The difference between $H^{\pm\pm}$ and H^\pm masses is dictated by the coupling λ_4 of the scalar potential. For a positive λ_4 , the $H^{\pm\pm}$ is lighter than H^\pm . The mass difference ΔM^2 is

$$\Delta M^2 = M_{H^\pm}^2 - M_{H^{\pm\pm}}^2 \sim \frac{\lambda_4}{2} v_\Phi^2 + \mathcal{O}(v_\Delta^2). \quad (2.14)$$

Throughout our analysis, we consider the mass hierarchy $M_{H^{\pm\pm}} < M_{H^\pm}$. Among the neutral Higgs fields, we identify h^0 as the SM Higgs with mass $M_{h^0} = 125$ GeV. The mass of h^0 is primarily decided by λ , where the mass of H^0 is primarily decided by M_Δ . The neutral Higgs mixing angle α is very small, and hence, $\cos \alpha \simeq 1$. On the other hand, the charged Higgs and CP odd Higgs mixing angles $\tan \beta_\pm$ and $\tan \beta_0$ being proportional v_Δ/v_Φ , is very small, $\tan \beta \sim 10^{-3}$. Note that, the mass square difference between H^\pm and H^0 in the limit $v_\Delta < v_\Phi$ is

$$M_{H^0}^2 - M_{H^\pm}^2 \sim \lambda_4 \frac{v_\Phi^2}{4} + \mathcal{O}(v_\Delta^2) \quad (2.15)$$

Therefore, the mass difference between $M_{H^{\pm\pm}}$, M_{H^\pm} and the mass difference between M_{H^0} , M_{H^\pm} are almost similar, and dictated by the same set of parameters λ_4 , and electroweak vev v_Φ . The mass square difference between H^0 and A^0 is extremely small, as this is proportional to the triplet vev,

$$M_{H^0}^2 - M_{A^0}^2 \sim 2v_\Delta^2(\lambda_2 + \lambda_3) - \frac{4}{\sqrt{2}}\mu v_\Delta. \quad (2.16)$$

We denote the mass difference between H^0 and A^0 by $M_{H^0} - M_{A^0} \sim \delta M \sim v_\Delta$, and the mass difference between H^\pm and H^0 by $M_{H^\pm} - M_{H^0} \sim \Delta M$. As we will discuss in the next subsequent sections, the later parameter is important for few of the decay modes that depend on charged Higgs and neutral Higgs mass splitting, and is one of the key parameter for our discussion.

Due to the non-trivial representations of Δ , the Higgs triplet has interactions with a number of SM fermions and gauge bosons. This opens up a number of possible decay modes that can be explored at the LHC, and at other future colliders. In the next section, we summarise the different direct experimental constraints on the charged Higgs states.

3 Decay Modes and Experimental Constraints

We assume the neutral Higgs H^0 and A^0 are more massive than the charged Higgs. Among the charged Higgs, H^\pm is heavier than $H^{\pm\pm}$. The doubly-charged Higgs boson $H^{\pm\pm}$ of this model can decay into the leptonic or bosonic states and gives unique signatures at high energy colliders. The partial decay widths and branching ratios of the $H^{\pm\pm}$ depend on the triplet vev v_Δ . For smaller triplet vev, the $H^{\pm\pm}$ predominantly decays into the same-sign leptonic states $H^{\pm\pm} \rightarrow l^\pm l^\pm$, whereas for larger v_Δ , the gauge boson mode $H^{\pm\pm} \rightarrow W^\pm W^\pm$ becomes dominant [20, 22, 23]. The relevant decay widths are calculated to be,

$$\Gamma(H^{\pm\pm} \rightarrow l_i^\pm l_j^\pm) = \Gamma_{l_i l_j} = \frac{M_H^{\pm\pm}}{(1 + \delta_{ij})8\pi} \left| \frac{M_{\nu_{ij}}}{v_\Delta} \right|^2, \quad M_\nu = Y_\Delta v_\Delta, \quad (3.1)$$

$$\Gamma(H^{\pm\pm} \rightarrow W^\pm W^\pm) = \Gamma_{W^\pm W^\pm} = \frac{g^2 v_\Delta^2}{8\pi M_{H^{\pm\pm}}} \sqrt{1 - \frac{4}{r_W^2}} [(2 + (r_W/2 - 1)^2)]. \quad (3.2)$$

Here, M_ν denotes the neutrino mass matrix, i, j are the generation indices, $\Gamma_{l_i l_j}$ and $\Gamma_{W^\pm W^\pm}$ are the partial decay widths for the $H^{\pm\pm} \rightarrow l_i^\pm l_j^\pm$, and $H^{\pm\pm} \rightarrow W^\pm W^\pm$ channels, respectively. The parameter r_W represents the ratio of $H^{\pm\pm}$ and the W gauge boson masses, $r_W = \frac{M_{H^{\pm\pm}}}{M_W}$.

Other than the doubly charged Higgs, the model also contains a singly charged Higgs. The singly charged Higgs H^\pm can decay to $l\nu$, WZ , Wh , $t\bar{b}$ final states. Additionally, for non-degenerate charged Higgs masses, and triplet vev v_Δ in between 10^{-6} GeV and 10^{-2} GeV, the cascade decay $H^\pm \rightarrow H^{\pm\pm}W^*$ can also become dominant. The partial width for the charged Higgs decaying into $H^{\pm\pm}W^{*-}$ have these following form:

$$\Gamma(H^\pm \rightarrow H^{\pm\pm}W^{*-}) = \frac{9g^4 M_{H^\pm}}{128\pi^3} \cos^2 \beta_\pm G\left(\frac{M_{H^{\pm\pm}}^2}{M_{H^\pm}^2}, \frac{M_W^2}{M_{H^\pm}^2}\right). \quad (3.3)$$

In the above β_\pm is the charged Higgs mixing angle. For the expression of the function G and other partial decay widths of H^\pm into two fermion, gauge bosons, see [26]. We show the branching ratio of $H^{\pm\pm}$ and H^\pm in Fig. 1, for two benchmark values of doubly charged Higgs mass, $M_{H^{\pm\pm}} = 247.3$ GeV and $M_{H^{\pm\pm}} = 894.02$ GeV, respectively. In the upper panel of Fig. 1, we show the variation of the branching ratios of doubly charged Higgs boson for the two chosen benchmark mass points. The lower panel shows the variation of the branching ratio of singly charged Higgs H^\pm into different channels. The lower panel has a different response with the increase of the doubly charged Higgs mass, which also implies the increase of the masses of different other charged and neutral Higgs states. From the top panel, this is evident, that there is hardly any change in the branching ratio of doubly charged Higgs for the variation of its mass, except a slight shift in the overlapping region of the two branching ratios. On the other hand in the lower panel, the scenario is completely different and one can easily see a huge variation in the branching ratio of the different decay channel of H^\pm due to the change in mass of the doubly charged Higgs. This happens because with the increase of the doubly charged Higgs mass the ratio $\frac{M_{H^{\pm\pm}}}{M_{H^\pm}} \rightarrow 1$, hence the decrement in the decay width of $H^+ \rightarrow H^{++}W^{*-}$ channel occurs due to the phase space suppression.

A number of searches have been proposed at the LHC to discover $H^{\pm\pm}$ using multilepton signatures. The searches in [22–24, 45] focussed on the pair and associated production with the $H^{\pm\pm}$ decaying into leptonic, gauge boson states. Below we discuss the existing constraints on $H^{\pm\pm}$ from LEP and LHC searches.

- Constraint from LEP-II: The search for doubly-charged Higgs boson $H^{\pm\pm}$ decaying into charged leptons have been performed at LEP-II. This constrains the mass $M_{H^{\pm\pm}} > 97.3$ GeV [47] at 95% C.L.
- Constraints from pair and associated production: Stringent constraint on $M_{H^{\pm\pm}}$ have been placed by the 13 TeV LHC searches. These searches analysed $H^{\pm\pm} \rightarrow l^\pm l^\pm$ channel. The CMS collaboration looked for different leptonic flavors including $ee, e\mu, e\tau, \mu\mu, \mu\tau$ and $\tau\tau$. In addition, the CMS searches also include the associated

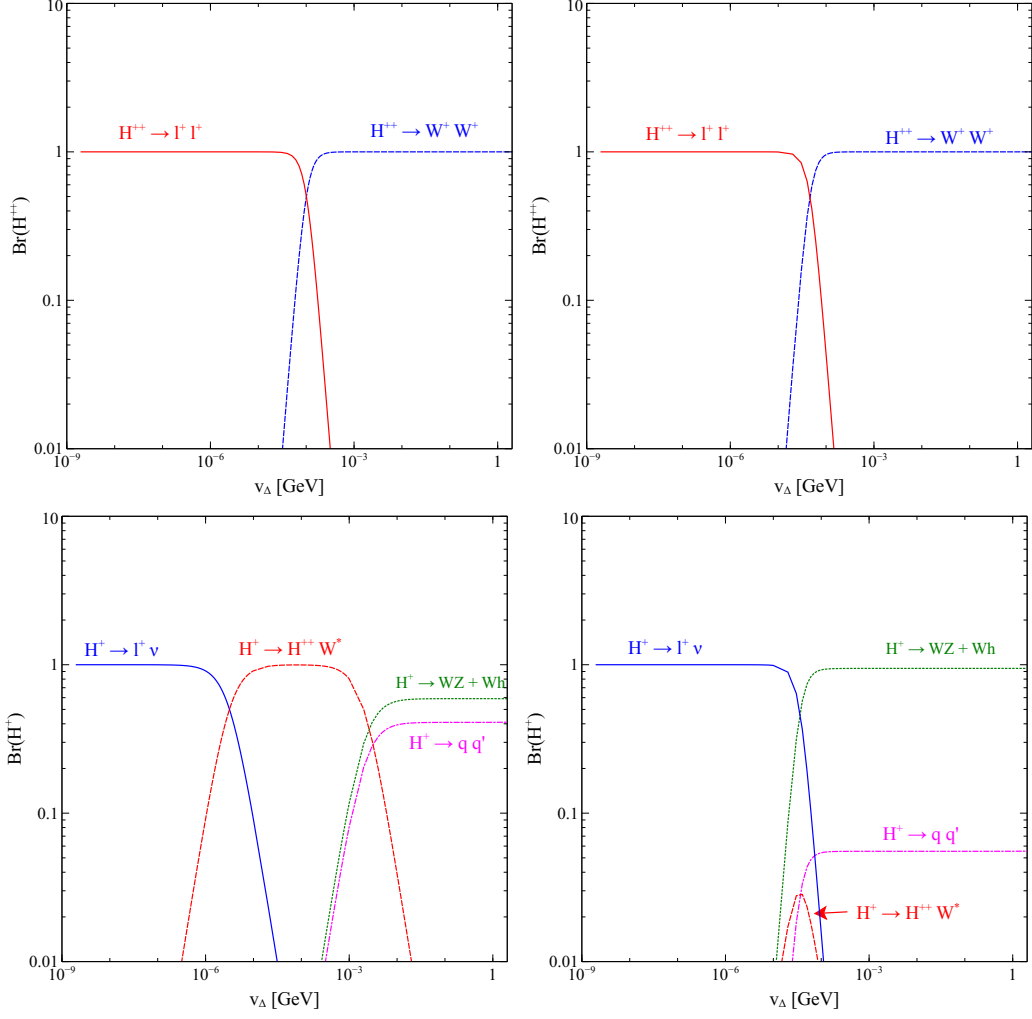


Figure 1. Upper panel: the branching ratios of $H^{\pm\pm}$ for masses $M_{H^{\pm\pm}} = 247.30$ GeV and $M_{H^{\pm\pm}} = 894.02$ GeV. Lower panel: branching ratios of H^{\pm} for the masses, $M_{H^{\pm}} = 250.35$ GeV and $M_{H^{\pm}} = 894.89$ GeV. The other relevant parameters are kept fixed at $\lambda_i = 0.1$ (for $i = 1$ to 4) and $\lambda = 0.52$.

production $pp \rightarrow H^{\pm\pm} H^{\mp}$ and the subsequent decays, $H^{\pm} \rightarrow l^{\pm} \nu$. This combined channel of pair-production and associated production gives the stringent constraint $M_{H^{\pm\pm}} > 820$ GeV [39] at 95% C.L for e, μ flavor. The realistic bound depends on the neutrino mass matrix [20]. Similar constraint from ATLAS searches have been placed on the mass of doubly charged Higgs, that takes into account only pair-production. The bound is $M_{H^{\pm\pm}} > 870$ GeV at 95% C.L [38]. Note that these limits are valid only for a small triplet vev $v_\Delta < 10^{-4}$ GeV. Additionally, ATLAS looked into the pair-production of doubly charged Higgs, with subsequent decays into gauge bosons, resulting in multi-lepton final states. The search in [54], have constrained the mass of doubly charged Higgs $M_{H^{\pm\pm}}$ in between 200-220 GeV at 95% C.L. This is valid

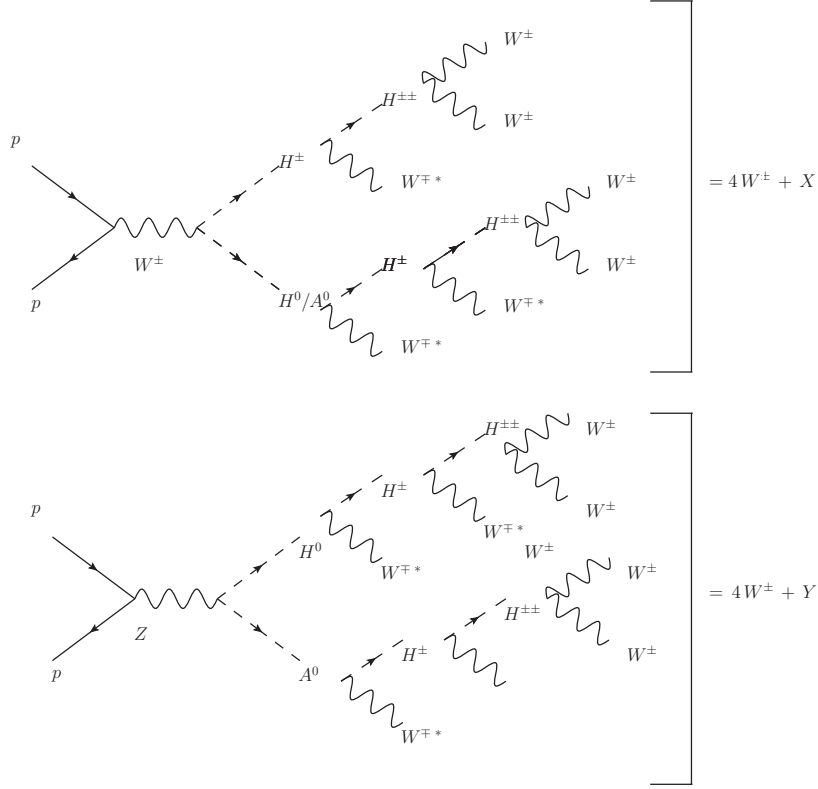


Figure 2. Feynman diagrams for $pp \rightarrow H^\pm H^0/A^0$, $pp \rightarrow H^0 A^0$, and the subsequent decays of $H^0/A^0 \rightarrow H^\pm W^{-*}$, $H^\pm \rightarrow H^{\pm\pm} W^{-*}$, and $H^{\pm\pm} \rightarrow W^\pm W^\pm$.

for the triplet vev $v_\Delta > 10^{-4}$ GeV, where the gauge boson decay is most dominant.

- Constraint from VBF: For larger values of the triplet vev $v_\Delta > 10^{-4}$ GeV, the leptonic branching ratio becomes smaller. Instead the decay mode $H^{\pm\pm} \rightarrow W^\pm W^\pm$ is dominant. Therefore the searches in vector boson fusion (VBF) become more important. A search for $pp \rightarrow jj H^{\pm\pm} \rightarrow jj W^\pm W^\pm$ at the 8 TeV LHC in the VBF channel sets a constraint on the triplet vev $v_\Delta \sim 25$ GeV for $M_{H^{\pm\pm}} \sim 300$ GeV [40]. This constraint has been updated [41] using 13 TeV data at the LHC. Such a large triplet vev is anyway excluded by the ρ parameter bound [19] in the minimal type-II seesaw model.

The above mentioned constraints imply that a large range of triplet vev $v_\Delta > 10^{-4}$ GeV exists, where low mass of $M_{H^{\pm\pm}} > 220$ GeV is still allowed. For lower triplet vev $v_\Delta < 10^{-4}$ GeV, the mass constraint is more conservative $M_{H^{\pm\pm}} > 870$ GeV. In our

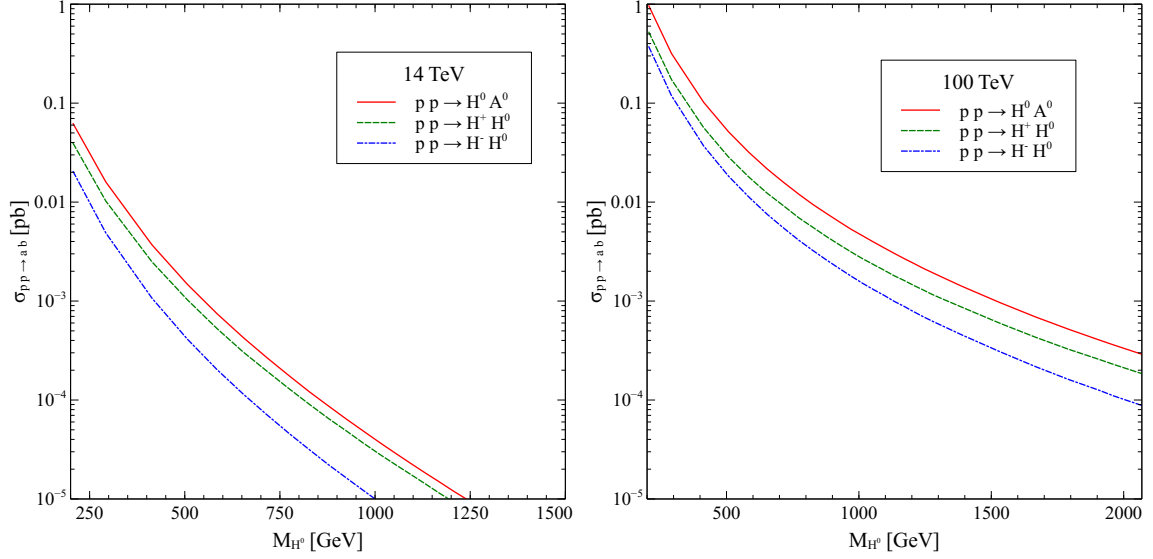


Figure 3. Left panel: cross-section for associated production $H^\pm H^0$, $H^0 A^0$ vs the mass of H^\pm . The c.m.energy is $\sqrt{s} = 14$ TeV. The other parameters are fixed at $\lambda_i = 0.1$ ($i = 1$ to 4), $\lambda = 0.52$, $v_\Delta = 10^{-3}$ GeV and μ has been varied between 2×10^{-3} GeV to 4.5×10^{-2} GeV to vary the mass of the particles. The production cross section for $H^+ A^0$ and $H^- A^0$ are same with $H^+ H^0$ and $H^- H^0$, respectively. Right panel: The same plot for higher c.m.energy $\sqrt{s} = 100$ TeV.

analysis of tetra-lepton signatures, we therefore choose both the lighter and heavier mass points.

4 Large triplet vev and same-sign tetra-lepton signature for $\sqrt{s} = 14$ TeV

We explore the tetra-lepton signature arising from a lighter charged Higgs and neutral Higgs decay. We consider associated production of H^\pm along-with H^0/A^0 . For triplet vev in between 10^{-5} GeV $< v_\Delta < 10^{-3}$ GeV, and assuming mass hierarchy between singly and doubly charged Higgs $M_{H^\pm} > M_{H^{\pm\pm}}$, the cascade decay of H^\pm into $H^{\pm\pm} W^*$ is predominant. In the same triplet vev region, $H^0/A^0 \rightarrow H^\pm W^*$ decay is also significantly large. We furthermore consider the gauge boson decay modes of $H^{\pm\pm} \rightarrow W^\pm W^\pm$, that has large branching ratio for $v_\Delta > 10^{-4}$ GeV and subsequent leptonic decay of the produced on-shell W^\pm . For the signal, therefore, the complete process is [53],

- $pp \rightarrow H^\pm H^0 / H^\pm A^0 \rightarrow H^{\pm\pm} W^{\pm*} H^\pm W^{\mp*} \rightarrow H^{\pm\pm} W^{\pm*} H^{\pm\pm} W^{\mp*} W^{\mp*} \rightarrow 4W^\pm + X$
- $pp \rightarrow H^0 A^0 \rightarrow H^\pm W^{\mp*} H^\pm W^{\mp*} \rightarrow H^{\pm\pm} W^{\pm*} H^{\pm\pm} W^{\mp*} W^{\mp*} W^{\mp*} \rightarrow 4W^\pm + Y$

The Feynman diagrams for these above two processes have been shown in Fig. 2. Note that this phenomenon of wrong sign leptons production occurs as Δ^0 can oscillate to $\Delta^{0\dagger}$ and vice versa. As a result, H^0 and A^0 , sharing the same final states, can mix together like in the $B^0 - \bar{B}^0$ system. Finally we can write the cross-section for these signals as:

- $\sigma(pp \rightarrow H^\pm H^0/A^0) \times F_1 \times \text{Br}(H^\pm \rightarrow H^{\pm\pm}W^{-*})^2 \times \text{Br}(H^0/A^0 \rightarrow H^\pm W^{-*}) \times \text{Br}(H^{\pm\pm} \rightarrow W^\pm W^\pm)^2$
- $\sigma(pp \rightarrow H^0 A^0) \times F_2 \times \text{Br}(H^0/A^0 \rightarrow H^\pm W^{-*})^2 \times \text{Br}(H^\pm \rightarrow H^{\pm\pm}W^{-*})^2 \times \text{Br}(H^{\pm\pm} \rightarrow W^\pm W^\pm)^2$

In the above $F_{1,2}$ are

$$F_1 = \frac{x^2}{1+x^2}, \quad F_2 = \frac{2+x^2}{2(1+x^2)} \times \frac{x^2}{2(1+x^2)}, \quad \text{with } x = \frac{\delta M}{\Gamma_{H^0/A^0}} = \frac{M_{H^0} - M_{A^0}}{\Gamma_{H^0/A^0}} \quad (4.1)$$

When the two decay widths Γ_{H^0} and Γ_{A^0} are nearly equal, i.e., $\Gamma_{H^0} \simeq \Gamma_{A^0}$. The generalisation of these two processes to the case of $\Gamma_{A^0} \neq \Gamma_{H^0}$ is

- $\sigma(pp \rightarrow H^\pm H^0/A^0) \times G_1 \times \text{Br}(H^\pm \rightarrow H^{\pm\pm}W^{-*})^2 \times \text{Br}(H^0/A^0 \rightarrow H^\pm W^{-*}) \times \text{Br}(H^{\pm\pm} \rightarrow W^\pm W^\pm)^2$
- $\sigma(pp \rightarrow H^0 A^0) \times G_2 \times \text{Br}(H^0/A^0 \rightarrow H^\pm W^{-*})^2 \times \text{Br}(H^\pm \rightarrow H^{\pm\pm}W^{-*})^2 \times \text{Br}(H^{\pm\pm} \rightarrow W^\pm W^\pm)^2$

where G_1 and G_2 have the following forms:

$$G_1 = \frac{x^2 + y^2}{2(1+x^2)}, \quad G_2 = \frac{2+x^2-y^2}{2(1+x^2)} \times \frac{x^2+y^2}{2(1+x^2)}, \quad \text{with } x = \frac{\delta M}{\Gamma},$$

$$\Gamma = \frac{\Gamma_H^0 + \Gamma_A^0}{2}, \quad \text{and } y = \frac{\Gamma_H^0 - \Gamma_A^0}{\Gamma_H^0 + \Gamma_A^0} \quad (4.2)$$

Note that, to compute the tetra-lepton signature, one needs to take into account the leptonic branching ratios from W . In our analysis, we consider both the $W \rightarrow l\nu$, with $l = e, \mu$, as well as $W \rightarrow \tau\nu$, with the leptonic decays of τ included. To compute the cross-section, we implement the model in FeynRules(v2.3) [55]. The UFO output is then fed into MadGraph5_aMC@NLO(v2.6) [56] that generates the parton-level events. We use the default pdf NNPDF23LO1 [57] for computation. We perform parton showering and hadronization with Pythia8 [58] and analyse the HepMC [59] event files. The above cross-sections $pp \rightarrow H^\pm H^0$ and $pp \rightarrow H^0 A^0$ depend on the masses of the neutral and charged Higgs. We therefore show the variation of associated production cross-section of $pp \rightarrow H^\pm H^0/A^0$ and $pp \rightarrow H^0 A^0$ with the mass of H^0 in Fig. 3. For c.m.energy $\sqrt{s} = 14$ TeV, the cross-section for $pp \rightarrow H^0 A^0$ varies in between 1 – 70 fb, for neutral Higgs mass between 200 – 500 GeV. For $pp \rightarrow H^+ H^0/A^0$, the cross-section is very similar, only lower than by a factor of $\mathcal{O}(1.5)$. For $pp \rightarrow H^- H^0/A^0$, cross-section is smaller due to the parton distribution function. In addition, we also show the production cross-section for a future pp collider, with c.m.energy $\sqrt{s} = 100$ TeV. As is evident from the right panel of Fig. 3, the production cross-section is quite large for higher c.m.energy, and multi-TeV Higgs mass can be probed.

Note that the production cross-sections for $pp \rightarrow H^\pm H^0/A^0$ depends on both the parameters λ_4 and the triplet vev v_Δ . For a fixed value of μ , the triplet vev primarily governs the masses of the Higgs $H^\pm, H^0/A^0$, while the parameter λ_4 determines their mass difference. In the left panel of Fig. 4, we show the variation of production cross section

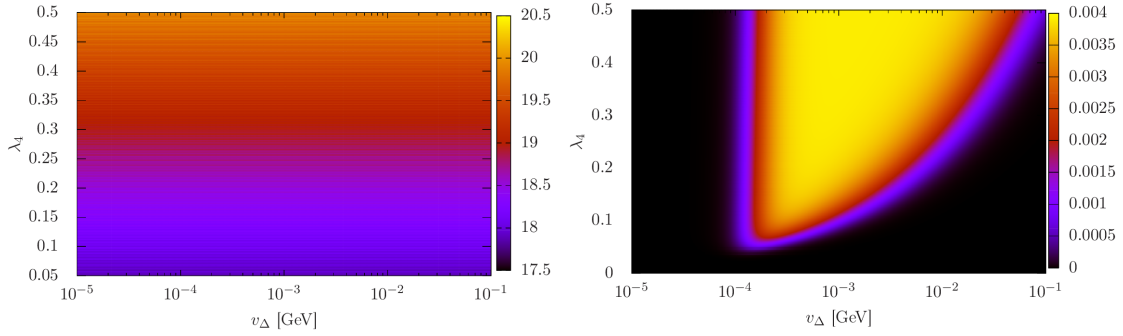


Figure 4. Left panel: cross section in fb for the channel $pp \rightarrow H^+H^0$ for the c.m.energy $\sqrt{s} = 14$ TeV ($M_{A^0} = 253$ GeV). Right panel: Product of branching ratios $\text{Br}(H^\pm \rightarrow H^{\pm\pm}W^{-*})^2 \times \text{Br}(H^0/A^0 \rightarrow H^\pm W^{-*}) \times \text{Br}(H^{\pm\pm} \rightarrow W^\pm W^\pm)^2 \times \text{Br}(W^\pm \rightarrow \ell\nu)^4$ for the process $pp \rightarrow H^\pm H^0/A^0$ with mass of A^0 being fixed as $M_{A^0} = 253$ GeV. For the second process $pp \rightarrow H^0/A^0$, behaviour of the product of branching ratio will be same.

for the process $pp \rightarrow H^+H^0$ in the $v_\Delta - \lambda_4$ plane for a benchmark value of neutral Higgs, $M_{H^0} \sim 253$ GeV. For the process $pp \rightarrow H^-H^0$, the plot is very similar, only the production cross section is relatively smaller by a factor of two. The channel $pp \rightarrow H^0A^0$ has the largest cross-section, larger than $pp \rightarrow H^+H^0$ by almost a factor of $\mathcal{O}(1.4 - 1.7)$. Since λ_4 has a very nominal effect on the mass splitting of H^0, A^0 , the cross-section of this channel is almost fixed in the entire plane of $\lambda_4 - v_\Delta$, and thus does not vary.

The doubly, singly charged, and neutral Higgs bosons will decay through a number of subsequent decay modes, leading to the same-sign tetra-lepton final states. The two key parameters are again triplet vev v_Δ and the coupling λ_4 . Since a number of branching ratios are involved in the same-sign tetra-lepton process, we show the product of these branching ratios. In the right panel of Fig. 4, we show the variation of the product of branching ratios $\text{Br}(H^\pm \rightarrow H^{\pm\pm}W^{-*})^2 \times \text{Br}(H^0/A^0 \rightarrow H^\pm W^{-*}) \times \text{Br}(H^{\pm\pm} \rightarrow W^\pm W^\pm)^2 \times \text{Br}(W^\pm \rightarrow \ell\nu)^4$ for the process $pp \rightarrow H^\pm H^0/A^0$ in the $v_\Delta - \lambda_4$ plane. From the top panel of Fig. 1, it is evident that the doubly charged Higgs $H^{\pm\pm}$ decays predominantly to same sign $W^\pm W^\pm$ state. For smaller range of the triplet vev it entirely decays to $l^\pm l^\pm$ final state. This is reflected in Fig. 4, where there is a sharp change in branching ratio around 10^{-4} GeV. The product goes to zero in the left side of this line (as shown by the black region). In the right side of this line, the product can be large, as indicated by the colour bar. We stress that, the product of the branching ratios has a significantly large value for a wide range of the triplet vev, 10^{-4} GeV $< v_\Delta < 10^{-2}$ GeV. Therefore, in this region, there will be handful of events for same-sign tetra-lepton final states, that can be tested at LHC. In the next section, we will see how this large range of triplet vev shrinks to a very narrow range for higher masses of the charged and neutral Higgs. This occurs due to significant change in branching ratios of the channel $H^\pm \rightarrow H^{\pm\pm}W^{-*}$ for the same value of λ_4 .

In Fig. 5, we show the variation of number of events for the same-sign tetra-lepton signature, where we consider integrated luminosity $\mathcal{L} = 3000 \text{ fb}^{-1}$. This has been obtained by folding the production cross-section with the overall branching ratio, and integrated

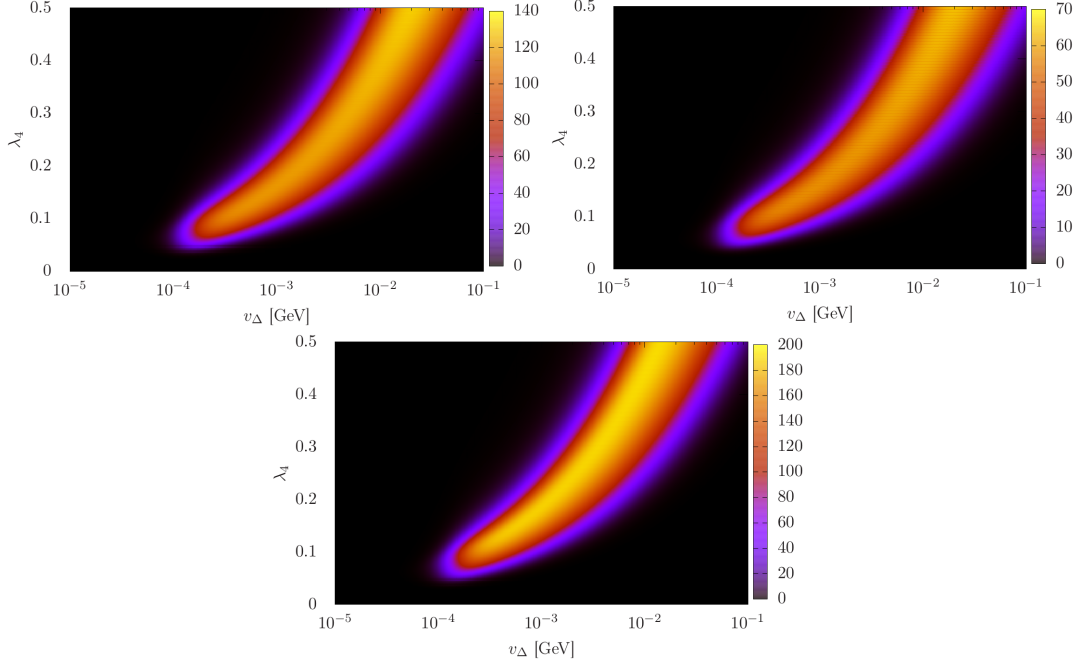


Figure 5. This plot represents number of same-sign tetralepton events for mass $M_{H^0} \sim M_{A^0} = 253$ GeV. Left figure of upper panel: number of same-sign tetralepton events $\ell^+ \ell^+ \ell^+ \ell^+ + X$ from $pp \rightarrow H^+ H^0 / A^0$ followed by subsequent decays of H^+, H^0, A^0 . Right figure of upper panel: number of same-sign tetralepton events $\ell^- \ell^- \ell^- \ell^- + X$ from $pp \rightarrow H^- H^0 / A^0$ and subsequent decays. Lower panel: number of same-sign tetralepton events $\ell^+ \ell^+ \ell^+ \ell^+ + Y$ or $\ell^- \ell^- \ell^- \ell^- + Y$ from $pp \rightarrow H^0 A^0$ and subsequent decays. For the doubly charged Higgs, we consider $H^{\pm\pm} \rightarrow W^\pm W^\pm$ decay mode. The c.m.energy $\sqrt{s} = 14$ TeV and we consider luminosity $\mathcal{L} = 3000 \text{ fb}^{-1}$. For this range of λ_4 , the masses of H^\pm and $H^{\pm\pm}$ varies at most by $M_{H^0} - M_{H^{++}} \sim 32$ GeV and $M_{H^0} - M_{H^+} \sim 15$ GeV respectively.

luminosity. We also implement few basic cuts at the pythia level. These are $p_T(e^\pm/\mu^\pm) > 10$ GeV, $|\eta(e^\pm/\mu^\pm)| < 2.5$. We obtain a cut-efficiency $c_{eff} = 0.62$ for $M_{H^0} = 253$ GeV, that we include in our calculation of total number of events. We consider the processes $pp \rightarrow H^+ H^0 / A^0$ (top left), $pp \rightarrow H^- H^0 / A^0$ (top right) and $pp \rightarrow H^0 A^0$ (bottom). To calculate the number of events we followed the prescription given at the beginning of Section 4. As we can see from the bottom left plot of Fig. 1, that for the low mass range of the particle spectrum, the channel $H^\pm \rightarrow H^{\pm\pm} W^* \rightarrow \ell^+ \ell^+ W^+ + c.c.$ has 100% branching ratio for a wide range of triplet vev. Hence in all these three plots, we get a reasonable number of events for triplet vev $v_\Delta \sim 10^{-4} - 10^{-1}$ GeV. As exhibited in Fig. 3, the cross section for the different final states have the following hierarchies $\sigma(pp \rightarrow H^0 A^0) > \sigma(pp \rightarrow H^+ H^0 / A^0) > \sigma(pp \rightarrow H^- H^0 / A^0)$. The same hierarchy also translates in the number of events. All the three plots have a similar kind of morphology in the $v_\Delta - \lambda_4$ plane and the nature of the variation of the number of events can be understood in the following way. Since we are considering $H^{\pm\pm} \rightarrow W^\pm W^\pm$ channel which start contributing when triplet vev is $v_\Delta > 10^{-4}$ GeV, so the number of events $N_{evt} > 5$ starts around this region of triplet vev.

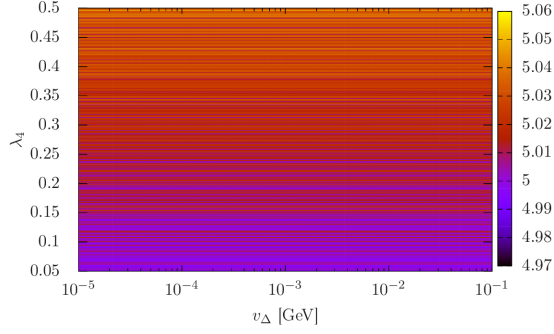


Figure 6. Cross section in fb for the channel $pp \rightarrow H^+H^0$ for the mass $M_{A^0} = 900$ GeV. We consider c.m.energy $\sqrt{s} = 100$ TeV.

As shown in Fig. 4, the cross section increases with larger λ_4 , while the branching ratio for the channel $H^\pm \rightarrow H^{\pm\pm}W^{-*}$ decreases (bottom right plot of Fig. 1) for larger triplet vev, leading to the specific variation of the number of events shown in 5.

5 Inclusive same-sign tetra-lepton signature for $\sqrt{s} = 100$ TeV

We consider heavier Higgs, and analyse its discovery prospect at a future pp collider that can operate with c.m.energy $\sqrt{s} = 100$ TeV. Due to the suppression from a number of branching ratios, observation of same-sign tetra-lepton final states will be beyond the scope of 13 TeV LHC. However, this can easily be observed in a future collider with higher c.m.energy. As a benchmark sample, we consider neutral Higgs mass $M_{H^0/A^0} = 900$ GeV, and variation of doubly charged Higgs of mass at most by 5 GeV from M_{H^0/A^0} . The chosen value of the doubly charged Higgs mass is consistent with the constraints from 13 TeV LHC searches for the entire range of triplet vev $v_\Delta \sim 10^{-9} - 1$ GeV. Near the triplet vev $v_\Delta \sim 10^{-4}$, both the di-lepton and gauge boson modes will substantially contribute. We therefore cover a large range of triplet vev v_Δ , and consider the doubly charged Higgs decaying into both the same-sign di-lepton, and gauge boson modes. Hence, in addition to the gauge bosons, discussed in Sec. 4, the total cross-section also contains the following contribution from di-lepton decay mode,

- $\sigma(pp \rightarrow H^\pm H^0/A^0) \times G_1 \times \text{Br}(H^\pm \rightarrow H^{\pm\pm}W^{-*})^2 \times \text{Br}(H^0/A^0 \rightarrow H^\pm W^{-*}) \times \text{Br}(H^{\pm\pm} \rightarrow \ell^\pm \ell^\pm)^2$
- $\sigma(pp \rightarrow H^0 A^0) \times G_2 \times \text{Br}(H^0/A^0 \rightarrow H^\pm W^{-*})^2 \times \text{Br}(H^\pm \rightarrow H^{\pm\pm}W^{-*})^2 \times \text{Br}(H^{\pm\pm} \rightarrow \ell^\pm \ell^\pm)^2$

In the above, $l = e, \mu, \tau$, and we finally consider the leptonic branching ratios of τ , while calculating the number of events. The functions $G_{1,2}$ have been described in Section. 4. We show the variation of cross-section in Fig. 6. The cross-section for the mass $M_{A^0} = 900$ GeV varies around 5 fb. We next show the variation of the product of branching ratios in Fig. 7 for heavier charged and neutral Higgs. For triplet vev smaller than $v_\Delta < 10^{-4}$ GeV, the

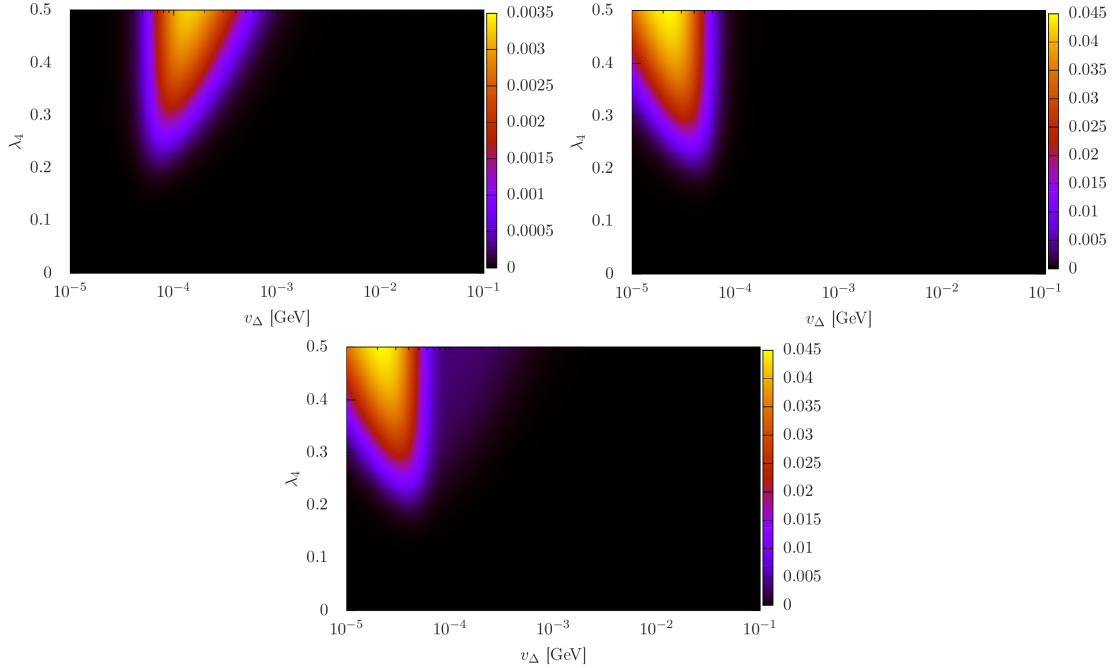


Figure 7. Upper panel: this represents the product of branching ratios $\text{Br}(H^\pm \rightarrow H^{\pm\pm}W^{-*})^2 \times \text{Br}(H^0/A^0 \rightarrow H^\pm W^{-*}) \times \text{Br}(H^{\pm\pm} \rightarrow W^\pm W^\pm)^2 \times \text{Br}(W^\pm \rightarrow \ell\nu)^4$ (left figure), $\text{Br}(H^\pm \rightarrow H^{\pm\pm}W^{-*})^2 \times \text{Br}(H^0/A^0 \rightarrow H^\pm W^{-*}) \times \text{Br}(H^{\pm\pm} \rightarrow \ell^\pm \ell^\pm)^2$ (right figure). Lower panel: the sum of these two products of branching ratios for the process $pp \rightarrow H^\pm H^0/A^0$ with mass of A^0 being fixed as $M_{A^0} = 900$ GeV. For the process $pp \rightarrow H^0 A^0$, the product of branching ratio is very similar.

doubly charged Higgs $H^{\pm\pm} \rightarrow l^\pm l^\pm$ is dominant, while around 10^{-4} GeV, both the gauge boson mode and di-lepton are dominant. For a heavier singly charged Higgs, the branching ratio for $H^\pm \rightarrow H^{\pm\pm}W^{-*}$ decay channel is large for a large value of λ_4 . Note that, for $\lambda_4 \sim 0.1$, the branching ratio becomes more than 1% in a very small range of the triplet vev (see Fig. 1). This in turns has large effect on the total branching ratio, and is clearly visible in all the three plots of Fig. 7. The region in v_Δ , in which the overall branching ratio is larger than 0.5% is now considerably smaller. The left plot in the top panel represents the overall branching ratio with only $H^{\pm\pm} \rightarrow W^\pm W^\pm$ decay included. The plot in the right panel shows the total branching ratio for $H^{\pm\pm} \rightarrow l^\pm l^\pm$. The product of the branching ratio is smaller for the case of $H^{\pm\pm} \rightarrow W^\pm W^\pm$ due to additional suppression from $\text{Br}(W^\pm \rightarrow \ell^\pm \nu)^4$. In the lower panel, we show the sum of these two branching ratios. The higher values of the product of the branching ratios is governed by $H^{\pm\pm} \rightarrow l^\pm l^\pm$ decay mode (relevant for $v_\Delta \lesssim 10^{-4}$ GeV). More explicitly we show the $H^{\pm\pm} \rightarrow W^\pm W^\pm$ dominated branching ratio by the blueish region, and $H^{\pm\pm} \rightarrow l^\pm l^\pm$ dominated branching ratio by yellowish region. The total cross-section has been computed by folding the branching ratios with the cross-section shown in Fig. 6. In addition, we also include few preliminary cuts, $p_T(e^\pm/\mu^\pm) > 10$ GeV, $|\eta(e^\pm/\mu^\pm)| < 2.5$. For $M_{H^0} = 900$ GeV and neutrino oscillation parameters to their best fit values[1], we obtain the cut-efficiencies $c_{eff} = 0.64$ in $H^{\pm\pm} \rightarrow l^\pm l^\pm$ mode and

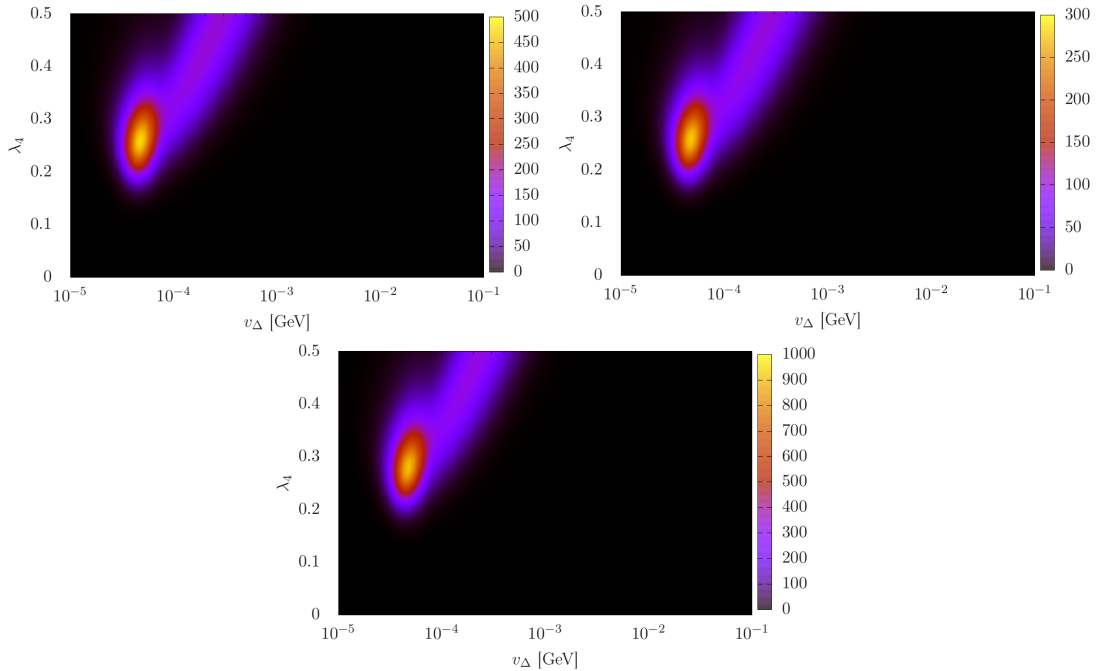


Figure 8. These figures represent number of events for mass $M_{A^0}/M_{H^0} = 900$ GeV. Upper panel: number of same-sign tetralepton events $\ell^+\ell^+\ell^+\ell^+ + X$ from $pp \rightarrow H^+H^0/A^0$ and subsequent decays (left), number of same-sign tetralepton events $\ell^-\ell^-\ell^-\ell^- + X$ from $pp \rightarrow H^-H^0/A^0$ and subsequent decays (right). Lower panel: number of same-sign tetralepton events $\ell^+\ell^+\ell^+\ell^+ + Y$ or $\ell^-\ell^-\ell^-\ell^- + Y$ from $pp \rightarrow H^0A^0$ and subsequent decays. We consider luminosity $\mathcal{L} = 30 \text{ ab}^{-1}$. For this range of λ_4 , the masses of H^\pm and $H^{\pm\pm}$ varies at most by $M_{H^0} - M_{H^{\pm\pm}} \sim 8.4 \text{ GeV}$ and $M_{H^0} - M_{H^\pm} \sim 4.2 \text{ GeV}$ respectively.

$c_{eff} = 0.62$ in $H^{\pm\pm} \rightarrow W^\pm W^\pm$ mode, that have been included in this analysis.

In Fig. 8, we present the number of events for heavier doubly charged Higgs, charged and neutral Higgs (~ 900 GeV). In all the three plots which correspond to $pp \rightarrow H^+H^0/A^0$, $pp \rightarrow H^-H^0/A^0$ and $pp \rightarrow H^0A^0$ processes, its possible to achieve a significantly large number of events in a very narrow region indicated by the yellow patch. This is in contrary to the low mass range, discussed in the previous section, where we get reasonable number of events for a wider range of triplet vev. Fig. 9 represents the variation of the total number of events for tetra leptons with either +ve or -ve sign of the leptons. The left panel shows the variation of the sum of the number of events ($l^+l^+l^+l^+ + l^-l^-l^-l^-$) for the low mass of the particles and its shape is exactly similar as discussed before (see Fig. 5). The figure in the right panel shows the events for higher mass and also has the similar shape as displayed in Fig. 8.

6 Conclusion

The type-II seesaw model is one of the most simplest models of neutrino mass generation, where the model is extended by an additional triplet scalar field. Due to an extended Higgs

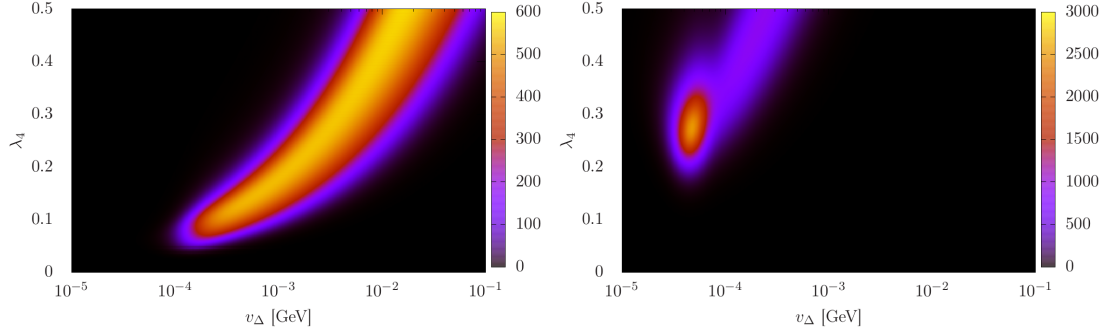


Figure 9. Total number of same-sign tetralepton events ($\ell^+\ell^+\ell^+\ell^+ + \ell^-\ell^-\ell^-\ell^-$) for both the cases $M_A^0 = 253$ GeV (left figure) and $M_{A^0} = 900$ GeV (right figure).

sector, and mixing between SM doublet scalar field and triplet scalar, the model contains few additional Higgs fields, including doubly charged and singly charged Higgs fields, as well as, CP even and odd neutral Higgs fields. In this work, we consider a type-II seesaw model for neutrino mass generation, and analyse an unique same-sign tetra-lepton signature at pp colliders. This arises from the associated production of Higgs fields $H^\pm H^0, H^0 A^0$, and the subsequent decay of neutral Higgs field into a singly charged Higgs state, and the decay of a singly charged field into a doubly charged Higgs state. More precisely, for non-degenerate Higgs masses, and for an intermediate triplet vev v_Δ in between 10^{-5} GeV $< v_\Delta < 10^{-2}$ GeV, the neutral and charged Higgs H^0, A^0, H^\pm decay predominantly to $H^0/A^0 \rightarrow H^\pm W^*$, and $H^\pm \rightarrow H^{\pm\pm} W^*$. The subsequent decays of $H^{\pm\pm}$ either to same-sign di-leptons, or to same-sign gauge bosons lead to the same-sign tetra-lepton final states. We analyse this signature for a pp collider, taking into account two different c.m.energies, $\sqrt{s} = 14$ TeV, and $\sqrt{s} = 100$ TeV. In our analysis, we choose those benchmark mass points, that are consistent with the present limits from 13 TeV LHC. In particular, for the lower c.m.energy, we explore the tetra-lepton signatures from a lighter Higgs state, and for higher c.m.energy, we consider a heavier Higgs states.

As an illustrative example, we first consider a large triplet vev $v_\Delta > 10^{-5}$ GeV, and a benchmark mass with $M_{H^0, A^0} = 253$ GeV. We vary the mass difference between doubly charged Higgs and charge neutral Higgs by at most 5 GeV. In this region of triplet vev, the gauge boson decay mode of $H^{\pm\pm}$ is pre-dominant. The associated production cross-section $pp \rightarrow H^+ H^0$ varies in between $\sigma \sim 17 - 20$ fb. The product of different branching ratios become maximal in a region $v_\Delta \sim 10^{-4}$ GeV $- 10^{-2}$ GeV. To analyse the signal events, we implement few basic cuts, for which we get a cut efficiency $c_{eff} = 0.6$. With integrated luminosity of $\mathcal{L} = 3000$ fb $^{-1}$, we find that a doubly charged Higgs of mass around 257 GeV can lead to 600 number of events at the future upgrade of LHC.

Additionally, we also consider heavier neutral, and doubly charged Higgs, for which tetra-lepton signature can be observed in a pp collider with higher c.m.energy. For illustration, we consider the mass $M_{H^0, A^0} = 900$ GeV, and vary the masses of doubly and singly charged Higgs at most by $M_{H^\pm} - M_{H^{\pm\pm}} \sim 5$ GeV. We explore the signal sensitivity for

this benchmark point at 100 TeV pp collider. We consider both the di-lepton and gauge boson decay modes of the doubly charged Higgs. For heavier mass, the branching ratio of $H^\pm \rightarrow H^{\pm\pm}W^*$ is large for a very large λ_4 . We find that the production cross-section of $pp \rightarrow H^+H^0$ varies nominally $\sigma \sim 5$ fb. We find that in a narrow region in $\lambda_4 - v_\Delta$ plane, the same-sign tetra-lepton events can be very large $N_{event} \sim \mathcal{O}(10^3)$.

Acknowledgments

MM acknowledges the support of the DST-INSPIRE research grant IFA14-PH-99, and the cluster facility of Institute of Physics (IOP), Bhubaneswar, India. EJC and MM thank the workshop 'NuHoRizon', held during March at HRI, India, where the work has been initiated.

References

- [1] P. F. de Salas, D. V. Forero, C. A. Ternes, M. Tortola and J. W. F. Valle, *Status of neutrino oscillations 2018: 3σ hint for normal mass ordering and improved CP sensitivity*, *Phys. Lett.* **B782** (2018) 633–640, [[1708.01186](#)].
- [2] S. Weinberg, *Baryon and Lepton Nonconserving Processes*, *Phys. Rev. Lett.* **43** (1979) 1566–1570.
- [3] F. Wilczek and A. Zee, *Operator Analysis of Nucleon Decay*, *Phys. Rev. Lett.* **43** (1979) 1571–1573.
- [4] P. Minkowski, *$\mu \rightarrow e\gamma$ at a Rate of One Out of 10^9 Muon Decays?*, *Phys. Lett.* **B67** (1977) 421–428.
- [5] R. N. Mohapatra and G. Senjanovic, *Neutrino Mass and Spontaneous Parity Violation*, *Phys. Rev. Lett.* **44** (1980) 912.
- [6] T. Yanagida, *Horizontal Symmetry and Masses of Neutrinos*, *Conf. Proc.* **C7902131** (1979) 95–99.
- [7] M. Gell-Mann, P. Ramond and R. Slansky, *Complex Spinors and Unified Theories*, *Conf. Proc.* **C790927** (1979) 315–321, [[1306.4669](#)].
- [8] J. Schechter and J. W. F. Valle, *Neutrino Masses in $SU(2) \times U(1)$ Theories*, *Phys. Rev.* **D22** (1980) 2227.
- [9] K. S. Babu, C. N. Leung and J. T. Pantaleone, *Renormalization of the neutrino mass operator*, *Phys. Lett.* **B319** (1993) 191–198, [[hep-ph/9309223](#)].
- [10] S. Antusch, M. Drees, J. Kersten, M. Lindner and M. Ratz, *Neutrino mass operator renormalization in two Higgs doublet models and the MSSM*, *Phys. Lett.* **B525** (2002) 130–134, [[hep-ph/0110366](#)].
- [11] M. Magg and C. Wetterich, *Neutrino Mass Problem and Gauge Hierarchy*, *Phys. Lett.* **B94** (1980) 61–64.
- [12] T. P. Cheng and L.-F. Li, *Neutrino Masses, Mixings and Oscillations in $SU(2) \times U(1)$ Models of Electroweak Interactions*, *Phys. Rev.* **D22** (1980) 2860.
- [13] G. Lazarides, Q. Shafi and C. Wetterich, *Proton Lifetime and Fermion Masses in an $SO(10)$ Model*, *Nucl. Phys.* **B181** (1981) 287–300.

- [14] R. N. Mohapatra and G. Senjanovic, *Neutrino Masses and Mixings in Gauge Models with Spontaneous Parity Violation*, *Phys. Rev.* **D23** (1981) 165.
- [15] R. Foot, H. Lew, X. G. He and G. C. Joshi, *Seesaw Neutrino Masses Induced by a Triplet of Leptons*, *Z. Phys.* **C44** (1989) 441.
- [16] A. Arhrib, R. Benbrik, M. Chabab, G. Moulataka, M. C. Peyranere, L. Rahili et al., *The Higgs Potential in the Type II Seesaw Model*, *Phys. Rev.* **D84** (2011) 095005, [[1105.1925](#)].
- [17] P. S. Bhupal Dev, D. K. Ghosh, N. Okada and I. Saha, *125 GeV Higgs Boson and the Type-II Seesaw Model*, *JHEP* **03** (2013) 150, [[1301.3453](#)].
- [18] D. Das and A. Santamaria, *Updated scalar sector constraints in the Higgs triplet model*, *Phys. Rev.* **D94** (2016) 015015, [[1604.08099](#)].
- [19] E. J. Chun, H. M. Lee and P. Sharma, *Vacuum Stability, Perturbativity, EWPD and Higgs-to-diphoton rate in Type II Seesaw Models*, *JHEP* **11** (2012) 106, [[1209.1303](#)].
- [20] E. J. Chun, K. Y. Lee and S. C. Park, *Testing Higgs triplet model and neutrino mass patterns*, *Phys. Lett.* **B566** (2003) 142–151, [[hep-ph/0304069](#)].
- [21] A. G. Akeroyd and M. Aoki, *Single and pair production of doubly charged Higgs bosons at hadron colliders*, *Phys. Rev.* **D72** (2005) 035011, [[hep-ph/0506176](#)].
- [22] P. Fileviez Perez, T. Han, G.-y. Huang, T. Li and K. Wang, *Neutrino Masses and the CERN LHC: Testing Type II Seesaw*, *Phys. Rev.* **D78** (2008) 015018, [[0805.3536](#)].
- [23] A. Melfo, M. Nemevsek, F. Nesti, G. Senjanovic and Y. Zhang, *Type II Seesaw at LHC: The Roadmap*, *Phys. Rev.* **D85** (2012) 055018, [[1108.4416](#)].
- [24] F. del Aguila and J. A. Aguilar-Saavedra, *Distinguishing seesaw models at LHC with multi-lepton signals*, *Nucl. Phys.* **B813** (2009) 22–90, [[0808.2468](#)].
- [25] S. Chakrabarti, D. Choudhury, R. M. Godbole and B. Mukhopadhyaya, *Observing doubly charged Higgs bosons in photon-photon collisions*, *Phys. Lett.* **B434** (1998) 347–353, [[hep-ph/9804297](#)].
- [26] M. Aoki, S. Kanemura and K. Yagyu, *Testing the Higgs triplet model with the mass difference at the LHC*, *Phys. Rev.* **D85** (2012) 055007, [[1110.4625](#)].
- [27] A. G. Akeroyd and H. Sugiyama, *Production of doubly charged scalars from the decay of singly charged scalars in the Higgs Triplet Model*, *Phys. Rev.* **D84** (2011) 035010, [[1105.2209](#)].
- [28] E. J. Chun and P. Sharma, *Search for a doubly-charged boson in four lepton final states in type II seesaw*, *Phys. Lett.* **B728** (2014) 256–261, [[1309.6888](#)].
- [29] F. del guila and M. Chala, *LHC bounds on Lepton Number Violation mediated by doubly and singly-charged scalars*, *JHEP* **03** (2014) 027, [[1311.1510](#)].
- [30] S. Banerjee, M. Frank and S. K. Rai, *Higgs data confronts Sequential Fourth Generation Fermions in the Higgs Triplet Model*, *Phys. Rev.* **D89** (2014) 075005, [[1312.4249](#)].
- [31] Z. Kang, J. Li, T. Li, Y. Liu and G.-Z. Ning, *Light Doubly Charged Higgs Boson via the WW^* Channel at LHC*, *Eur. Phys. J.* **C75** (2015) 574, [[1404.5207](#)].
- [32] Z.-L. Han, R. Ding and Y. Liao, *LHC Phenomenology of Type II Seesaw: Nondegenerate Case*, *Phys. Rev.* **D91** (2015) 093006, [[1502.05242](#)].

- [33] Z.-L. Han, R. Ding and Y. Liao, *LHC phenomenology of the type II seesaw mechanism: Observability of neutral scalars in the nondegenerate case*, *Phys. Rev.* **D92** (2015) 033014, [[1506.08996](#)].
- [34] K. S. Babu and S. Jana, *Probing Doubly Charged Higgs Bosons at the LHC through Photon Initiated Processes*, [1612.09224](#).
- [35] A. Crivellin, M. Ghezzi, L. Panizzi, G. M. Pruna and A. Signer, *Low- and high-energy phenomenology of a doubly charged scalar*, *Phys. Rev.* **D99** (2019) 035004, [[1807.10224](#)].
- [36] D. Borah, B. Fuks, D. Goswami and P. Poulou, *Investigating the scalar sector of left-right symmetric models with leptonic probes*, *Phys. Rev.* **D98** (2018) 035008, [[1805.06910](#)].
- [37] R. Padhan, D. Das, M. Mitra and A. Kumar Nayak, *Probing Doubly and Singly Charged Higgs at pp Collider HE-LHC*, [1909.10495](#).
- [38] ATLAS collaboration, M. Aaboud et al., *Search for doubly charged Higgs boson production in multi-lepton final states with the ATLAS detector using proton-proton collisions at $\sqrt{s} = 13$ TeV*, [1710.09748](#).
- [39] CMS collaboration, *A search for doubly-charged Higgs boson production in three and four lepton final states at $\sqrt{s} = 13$ TeV*, Tech. Rep. CMS-PAS-HIG-16-036, CERN, Geneva, 2017.
- [40] CMS collaboration, V. Khachatryan et al., *Study of vector boson scattering and search for new physics in events with two same-sign leptons and two jets*, *Phys. Rev. Lett.* **114** (2015) 051801, [[1410.6315](#)].
- [41] CMS collaboration, A. M. Sirunyan et al., *Observation of electroweak production of same-sign W boson pairs in the two jet and two same-sign lepton final state in proton-proton collisions at $\sqrt{s} = 13$ TeV*, [1709.05822](#).
- [42] S. Kanemura, K. Yagyu and H. Yokoya, *First constraint on the mass of doubly-charged Higgs bosons in the same-sign diboson decay scenario at the LHC*, *Phys. Lett.* **B726** (2013) 316–319, [[1305.2383](#)].
- [43] S. Kanemura, M. Kikuchi, K. Yagyu and H. Yokoya, *Bounds on the mass of doubly-charged Higgs bosons in the same-sign diboson decay scenario*, *Phys. Rev.* **D90** (2014) 115018, [[1407.6547](#)].
- [44] S. Kanemura, M. Kikuchi, H. Yokoya and K. Yagyu, *LHC Run-I constraint on the mass of doubly charged Higgs bosons in the same-sign diboson decay scenario*, *PTEP* **2015** (2015) 051B02, [[1412.7603](#)].
- [45] M. Mitra, S. Niyogi and M. Spannowsky, *Type-II Seesaw and Multilepton Signatures at Hadron Colliders*, [1611.09594](#).
- [46] D. K. Ghosh, N. Ghosh, I. Saha and A. Shaw, *Revisiting the high-scale validity of Type-II seesaw model with novel LHC signature*, [1711.06062](#).
- [47] DELPHI collaboration, J. Abdallah et al., *Search for doubly charged Higgs bosons at LEP-2*, *Phys. Lett.* **B552** (2003) 127–137, [[hep-ex/0303026](#)].
- [48] J.-F. Shen and Z.-X. Li, *Doubly charged Higgs bosons pair production through WW fusion at high-energy e^+e^- linear colliders*, *EPL* **111** (2015) 31001.
- [49] S. Blunier, G. Cottin, M. A. Daz and B. Koch, *Phenomenology of a Higgs triplet model at future e^+e^- colliders*, *Phys. Rev.* **D95** (2017) 075038, [[1611.07896](#)].

- [50] J. Cao and X.-Y. Tian, *Doubly and singly charged Higgs pair production at high-energy e^+e^- linear colliders*, *Int. J. Mod. Phys. A* **31** (2016) 1650056.
- [51] Y.-C. Guo, C.-X. Yue and Z.-C. Liu, *The signatures of doubly charged leptons in future linear colliders*, *J. Phys. G* **44** (2017) 085004, [[1611.08843](#)].
- [52] P. Agrawal, M. Mitra, S. Niyogi, S. Shil and M. Spannowsky, *Probing the Type-II Seesaw Mechanism through the Production of Higgs Bosons at a Lepton Collider*, *Phys. Rev. D* **98** (2018) 015024, [[1803.00677](#)].
- [53] E. J. Chun and P. Sharma, *Same-Sign Tetra-Leptons from Type II Seesaw*, *JHEP* **08** (2012) 162, [[1206.6278](#)].
- [54] ATLAS collaboration, M. Aaboud et al., *Search for doubly charged scalar bosons decaying into same-sign W boson pairs with the ATLAS detector*, *Eur. Phys. J. C* **79** (2019) 58, [[1808.01899](#)].
- [55] A. Alloul, N. D. Christensen, C. Degrande, C. Duhr and B. Fuks, *FeynRules 2.0 - A complete toolbox for tree-level phenomenology*, *Comput. Phys. Commun.* **185** (2014) 2250–2300, [[1310.1921](#)].
- [56] J. Alwall, R. Frederix, S. Frixione, V. Hirschi, F. Maltoni, O. Mattelaer et al., *The automated computation of tree-level and next-to-leading order differential cross sections, and their matching to parton shower simulations*, *JHEP* **07** (2014) 079, [[1405.0301](#)].
- [57] NNPDF collaboration, R. D. Ball, V. Bertone, S. Carrazza, L. Del Debbio, S. Forte, A. Guffanti et al., *Parton distributions with QED corrections*, *Nucl. Phys. B* **877** (2013) 290–320, [[1308.0598](#)].
- [58] T. Sjostrand, S. Mrenna and P. Z. Skands, *A Brief Introduction to PYTHIA 8.1*, *Comput. Phys. Commun.* **178** (2008) 852–867, [[0710.3820](#)].
- [59] M. Dobbs and J. B. Hansen, *The HepMC C++ Monte Carlo event record for High Energy Physics*, *Comput. Phys. Commun.* **134** (2001) 41–46.